Available online at www.sciencedirect.com

Journal of Photochemistry and Photobiology A: Chemistry 177 (2006) 129–143

Journal of Photochemistry and Photobiology A:Chemistry

www.elsevier.com/locate/jphotochem

Environmental remediation by an integrated microwave/UV illumination technique

IX. Peculiar hydrolytic and co-catalytic effects of platinum on the TiO_2 photocatalyzed degradation of the 4-chlorophenol toxin in a microwave radiation field

Satoshi Horikoshi [a], Atsushi Tokunaga [a], Natsuko Watanabe [a],
Hisao Hidaka [a,*], Nick Serpone [b,**,1]

[a] Frontier Research Center for the Global Environment Science, Meisei University, 2-1-1 Hodokubo, Hino, Tokyo 191-8506, Japan
[b] Dipartimento di Chimica Organica, Universita di Pavia, Via Taramelli 10, Pavia 27100, Italy

Received 13 October 2004; received in revised form 28 April 2005; accepted 16 May 2005

Abstract

The photocatalyzed degradation of the 4-chlorophenol toxin (4-CP) in aqueous naked TiO_2 and platinized TiO_2 suspensions simultaneously subjected to UV light and microwave radiation was revisited to examine the fate of this toxin in the microwave-assisted photocatalytic process by monitoring loss of total organic carbon (TOC; mineralization), formation of chloride ions (dechlorination of 4-CP), and identification of intermediates using HPLC and electrospray mass spectral (LC–MSD) techniques. Attempts are made to delineate microwave thermal and nonthermal factors that impinge on the degradation by comparing experimental results from microwave-generated heat versus results from a conventional (externally heated) thermally-assisted process, and from results in which the thermal factors were minimized by examining the degradative process at constant ambient temperature (25 °C). Possible microwave radiation effects on the Pt co-catalyst supported on TiO_2 were also probed through comparison of the degradation of 4-CP occurring on Pt/TiO_2 and on naked TiO_2 photocatalysts. Results suggest that, in a microwave radiation field, naked TiO_2 and Pt/TiO_2 particle surfaces interact with the microwaves. The degradation pathway exhibited characteristics of hydrolysis of reactants and intermediates. Nonthermal microwave effects play a role in the overall degradative process occurring in platinized TiO_2 dispersions. The possible nature of these unusual microwave effects is briefly discussed.

Keywords: Microwave-assisted photocatalysis; Soil contaminants; Microwave thermal effects; Microwave nonthermal effects; Environmental protection; Titanium dioxide; 4-Chlorophenol

---

1. Introduction

Chlorophenols constitute an important class of soil and water pollutants arising from their wide use as pesticides, herbicides, and as wood preservatives. In particular, 4-chlorophenol (4-CP), a representative of this class, is generated as a by-product of waste incineration. Accordingly, novel methodologies must be found or existing technologies must be improved to achieve efficient and total decomposition of such chlorinated phenols. Past investigations into the photocatalytic degradation of 4-CP and related derivatives in TiO_2 aqueous dispersions have emphasized (i) degradative pathways [1–11]; (ii) TiO_2-assisted electrochemistry [12,13]; (iii) degradative processes occurring on coupled TiO_2/CdS

---

[*] Corresponding author. Fax: +81 42 599 7785.
[**] Co-Corresponding author.
E-mail addresses: hidaka@epfc.meisei-u.ac.jp (H. Hidaka), nick.serpone@unipv.it, serpone@vax2.concordia.ca (N. Serpone).
[1] Professor Emeritus, Concordia University, Montreal, Canada.

1010-6030/$ – see front matter © 2005 Published by Elsevier B.V.
doi:10.1016/j.jphotochem.2005.05.018

systems [14], on incorporated co-catalysts as embodied by platinized titania (Pt/TiO_2) [15], and on polyoxometalates [16], together with; (iv) exploring laboratory-scale and large-scale applications of TiO_2 photocatalysis [17]. Studies have also been reported on reactors that saw TiO_2 particles supported on optical fibers [18,19].

In earlier reports, some characteristic features of microwave-assisted degradation reactions occurring on TiO_2 and some details of photooxidations and photoreductions were described for such systems as dyes (e.g. rhodamine-B), polymers, and surfactants [20,21], herbicides such as 2,4-dichlorophenoxyacetic acid [22], and endocrine disruptors such as bisphenol-A [23]. These reactions occurred at the TiO_2/water interface subjected to integrated UV light and microwave radiation. Several features of the microwave equipment were also tested. For instance, microwave radiation was used to power a microwave plasma electrodeless UV lamp [24–26].

Microwave radiation has found a niche in several synthetic chemical applications [27,28] and in the detoxification of an increasing number of chlorinated products [29–32]. Reports indicate that the decomposition dynamics are mostly governed by conventional microwave-generated heating (thermal) effects.

A characteristic feature of reactions that take place on TiO_2 originating from absorption of microwave radiation by the components of the reaction system involves microwave-generated thermal effects (i.e. caloric effects) and non-thermal (i.e. non-caloric) microwave effects [21–23,33]. In this regard, electron paramagnetic resonance (EPR) spectroscopic evidence showed that a greater number of $^{\bullet}OH$ radicals are produced in the microwave-assisted photocatalytic process (PD/MW) in aqueous TiO_2 dispersions [34]. The dynamics of the decomposition of organic pollutants by conventional TiO_2 photocatalysis were significant enhanced under microwave irradiation. It is worth pointing out that microwave radiation is not simply a source of heat that accelerates the degradation reactions. Other factors that we refer to as nonthermal factors are also at play.

The present study focused on three fundamental issues that were examined using the decomposition of a model compound of chlorine-containing toxins and dioxins, namely 4-chlorophenol, in naked TiO_2 and platinized titania (Pt/TiO_2) dispersions subjected to simultaneous irradiation by UV light and microwaves; 4-CP contains a phenolic OH group, a chlorine substituent and an aromatic ring. First we examined the microwave effects that might impact on the TiO_2 photocatalytic degradation process to provide further details on the mechanism of microwave-assisted decomposition. Next we probed the influence of Pt co-catalyst deposits supported on TiO_2 on the formation of intermediates, on the nature of the intermediates, on the dechlorination process, and on the formation of $^{\bullet}OH$ and $^{\bullet}OOH$ radicals when microwave radiation is also involved in Pt/TiO_2 photocatalysis. Finally, attempts were made to unravel the role of microwaves by a further examination of the possible implication of thermal (caloric) and nonthermal (non-caloric) microwave factors in the photocatalytic degradation of 4-CP.

2. Experimental

2.1. Chemicals and materials

Titanium dioxide was Degussa P-25 grade. High-purity grade 4-chlorophenol was purchased from Tokyo Kasei Kogyo Co. Ltd.

Platinized titanium dioxide particulates (Pt/TiO_2) were prepared by the photocatalytic deposition method [35] as modified by Harada et al. [36] and reported recently also by Radoiu et al. [32]. Thus, TiO_2 particles (P-25; 2 g loading) and 2-propanol (0.5 mL) were added to a 100 mL aqueous solution containing $H_2PtCl_6{\cdot}6H_2O$ (0.5 vol%; 0.02 mM); the pH of the dispersion was adjusted to pH 4.0 by addition of sodium acetate. The suspension was pre-purged with pure nitrogen gas and then irradiated with a 75 W low-pressure mercury lamp for 3 h at ambient temperature. The platinized TiO_2 particulates were separated by filtration, added to a dilute HCl solution (1 M, 200 mL), stirred for 1 h, re-filtered and repeatedly washed with deionized water until no more Cl^- ions were detected in the supernatant liquid. The sample was subsequently dried for ca. 2 days in a vacuum oven at 120 °C.

2.2. Characterization of the photocatalyst specimen

The amount of Pt loaded onto TiO_2 particles (ca. 0.29 wt.%) was determined with a Hitachi 4700 FE-SEM electron microscope using energy dispersive spectroscopy (EDS) for an average set of seven EDS data points employing an appropriate calibration method. The BET specific surface areas of P-25 TiO_2 and Pt/TiO_2 specimens were, respectively, 51.8 and 47.6 $m^2\ g^{-1}$. The bandgap energies were ascertained to be 3.10 eV for P-25 TiO_2 and 3.11 eV for Pt/TiO_2. Note that the anatase content remained at 83% (by X-ray diffraction methods) in these two specimens.

2.3. Experimental devices and procedures

Continuous microwave irradiation of the dispersions was achieved using a Shikoku Keisoku ZMW-003 apparatus consisting of a 2.45 GHz microwave generator (maximal power, 1.5 kW) fabricated by Shibaura Mechatronics Co., Ltd. (see microwave cavity A in Fig. 1 of [33]). Some details of the microwave system were reported previously [20–26,33,34]. The microwave power radiated from the magnetron was ca. 220 W measured using a power monitor.

A 30 mL air-equilibrated aqueous 4-CP solution (0.1 mM, initial pH 6.0) containing the photocatalyst particles (loading, 60 mg) was introduced into the reactor through a waveguide. Optimal low reflection of the MW radiation was

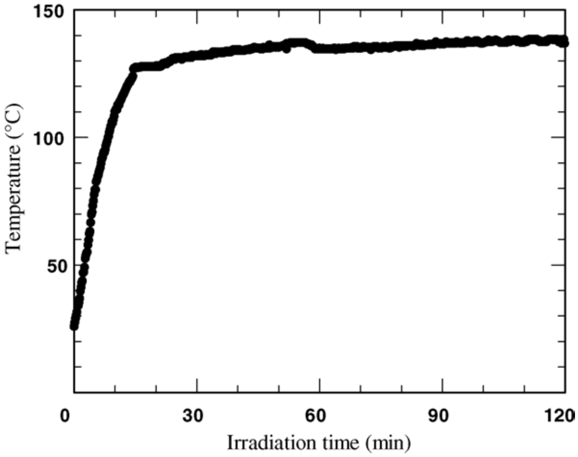

Fig. 1. Temporal increase of temperature in an aqueous 4-chlorophenol/TiO_2 dispersion subjected to UV light and a microwave radiation field.

achieved using the three-stub tuner. Unless otherwise noted, the UV irradiation source was a Toshiba 75 W low-pressure mercury lamp (irradiance ca. 0.3 mW cm^{-2}), whose UV radiation was fed to the 25 mL Pyrex cylindrical reactor ($\phi = 45$ mm × 290 mm; Taiatsu Techno® Co.; maximal pressure, 1 MPa; maximal temperature, 150 °C) by a fiber optic light-guide. The reactor was sealed with two Teflon rings and a stainless steel cap. The dispersion was continually stirred during irradiation.

2.4. Experimental degradation methodologies

Four different methodologies were examined to achieve the decomposition of the chlorophenol toxin. The first was photocatalytic degradation under UV light and microwave irradiation (PD/MW) of air-equilibrated 4-CP/TiO_2 or 4-CP–Pt/TiO_2 dispersions. The rate of change of temperature for the aqueous 4-CP/TiO_2 dispersion under these conditions is graphically illustrated in Fig. 1. The maximal temperature was 137 °C. The second method entailed the photocatalytic degradation of the toxin in 4-CP/TiO_2 and 4-CP–Pt/TiO_2 dispersions by UV irradiation alone (PD), whereas the third method involved the thermally-assisted photocatalytic degradation of 4-CP in naked TiO_2 and Pt/TiO_2 dispersions with UV light and externally applied conventional heat (PD/TH). The last method involved irradiation of the 4-CP/TiO_2 dispersion with microwaves only (MW). For the thermally-assisted PD/TH method, external heat was supplied by coating one part of the cylindrical photoreactor with a metallic film (MOCVD technique) on one side at the bottom of the reactor (applied voltage $\leq$100 V). The uncoated side was used to permit the 4-CP/TiO_2 or 4-CP–Pt/TiO_2 dispersions to be UV-irradiated. The rate of increase of temperature (error $\leq\pm$1 °C) and the pressure in the MW and PD/TH methods were maintained at the levels otherwise identical to those used for the PD/MW method.

2.5. Degradation of 4-CP at constant ambient temperature (25 °C)

To unravel the thermal (caloric) and nonthermal (non-caloric) microwave factors in the degradation processes, experiments were done at constant ambient temperature so as to diminish the thermal component of the microwave-generated heat. Accordingly, experiments were carried out by the PD/MW method and for the TiO_2 photocatalytic PD degradation using the microwave cavity B (Fig. 1 of [33]) in a dry-ice/hexane bath to maintain the ambient temperature of the dispersion reasonably constant at 25 ± 2 °C. These experiments are referred to as PD_{25} and PD/MW_{25}. For naked TiO_2 and Pt/TiO_2 catalytic systems, the PD/TH technique was compared to the PD/MW method. In the latter case, the thermal energy was supplied by the microwave radiation [20,33]. Pertinent results are discussed later in Sections 3.2 and 3.7. Microwave power was 550 ± 80 W, with the uncertainty established automatically by the amount of dry ice, which under our conditions absorbed no microwave radiation. Moreover, in these constant ambient temperature experiments, the Ushio 250 W mercury light source was used; it was located on top of the microwave oven emitting a light irradiance of 18 mW cm^{-2} that was fed to the reactor through the light wave-guide (fiber optic). The stronger light source was used for this occasion to enhance degradation and minimize temperature fluctuations during the experiments.

2.6. Analytical procedures

The time profiles of the disappearance of 4-chlorophenol and the intermediates produced during the degradation process were obtained by monitoring concentration changes using a JASCO liquid chromatograph (HPLC) equipped with a JASCO UV-2070 UV–vis diode array multi-wavelength detector and a JASCO Crestpak C-18S column; the eluent consisted of a mixed solution of CH_3CN and H_2O (1:4, v/v ratio) and 1.7 vol% of H_3PO_4 (pH 3.3). Because the UV absorption spectra of the degraded chlorophenol solution might easily be altered by intermediates produced during the decomposition process, the components of the reactant solution (irradiated or not) were timely separated by HPLC methods; the extent of disappearance of 4-CP and the formation and decay of intermediate species were established from the appropriate absorbance signals in the HPLC chromatograms.

The temporal changes in total organic carbon (TOC) in the degradation of 4-CP were assayed with a Shimadzu TOC-5000A analyser.

Carboxylic acid intermediates were detected employing a JASCO HPLC chromatograph and a Shodex OA System that comprised a RSpak KC-811 column and a Shodex OA kit for analysis of organic acids. The methodology incorporated a post-column derivatization procedure; spectroscopic detection was done at a wavelength of 445 nm.

The intermediates were also identified by direct injection into the mass spectral detector of an Agilent Technologies 1100 LC–MSD (electrospray ionization: API–ESI) system operated in the positive- and negative-ion modes (capillary voltage, 2800 V; dry gas temperature, 300 °C). The injected 10 μL volume of the sample solution was loaded using an Agilent Technologies 1100 auto-sampling device. The eluent was a solution of acetonitrile/water (1:1, v/v). The mass spectra were recorded by scanning the spectrometer from $m/z = 50$ to 400 at 0.3 mL min^{-1}.

3. Results and discussion

3.1. Overall photodegradation in TiO_2 dispersions

Aqueous solutions of 4-CP display absorption bands at 194 nm, 223 nm and 279 nm. Fig. 2a illustrates the temporal disappearance of 4-CP monitored at 279 nm by HPLC techniques that resulted from the four degradation methods employed to degrade the chloro-phenol (note that the rates of loss of the chlorophenol assayed at all three wavelengths were identical in all cases). The inset in Fig. 2a shows the HPLC pattern of 4-CP (retention time, RT = 16.4 min) and of the intermediates after 120 min of irradiation by the PD/MW method. A control experiment confirmed the 16.4 min HPLC signal to be that of 4-chlorophenol. Loss of UV absorption intensity in the HPLC chromatogram by the PD/MW method was more pronounced than by the PD and PD/TH methods indicating that ring opening of the aromatic ring was more prominent in the microwave-assisted photocatalyzed reaction. Conventional heating had no particular accelerating effect on the photocatalyzed PD degradation. Microwave irradiation (MW) of the 4-CP solution was inconsequential in the degradation of the chlorophenol. Except for the MW method, the extent of degradation of 4-CP after a 120 min irradiation period was 55% (PD/TH), 65% (PD) and 90% (PD/MW); this order roughly correlates with the approximate dynamics: PD/TH ($k \sim 0.01\ \mathrm{min}^{-1}$). PD ($k \sim 0.01\ \mathrm{min}^{-1}$) < PD/MW ($k \sim 0.02\ \mathrm{min}^{-1}$). Comparison of these data suggests that nonthermal effects of the microwave radiation are most likely responsible in promoting ring opening [21–23,33].

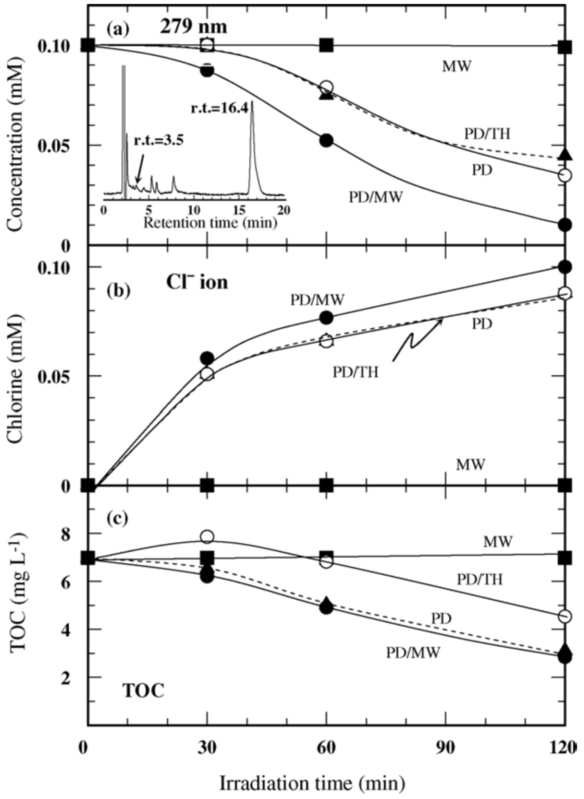

Fig. 2. (a) Temporal decrease of 4-chlorophenol concentration using UV absorption loss at 279 nm in the HPLC chromatogram; (b) time profiles of the formation of chloride ions, i.e. dechlorination of 4-CP; and (c) temporal loss of total organic carbon (TOC) during the degradation of a 4-chlorophenol solution by microwave irradiation (MW), photocatalyzed oxidation (PD), thermally-assisted photocatalyzed oxidation (PD/TH), and by an integrated microwave-assisted photocatalyzed degradation (PD/MW) in naked aqueous TiO_2 dispersions.

The temporal formation of Cl^- ions through dechlorination of 4-CP and the temporal loss of total organic carbon (TOC) on irradiation by the MW, PD, PD/TH and PD/MW methods are illustrated in Fig. 2b and c, respectively. Microwave irradiation alone had no effect on dechlorination of 4-CP and on the loss of TOC. Although the extent of dechlorination was complete, (100%) for PD/MW after 120 min, and nearly so for PD and PD/TH methods (92%), the first-order formation of Cl^- ions was identical for all three irradiation methods ($k \sim 0.025\ \mathrm{min}^{-1}$). For the loss of TOC (i.e. evolution of CO_2; mineralization) the PD/MW and PD methods displayed nearly identical behavior with ca. 58% of 4-CP mineralized compared to ca. 35% for the PD/TH route; zero-order dynamics were also identical in all three cases ($k \sim 0.04\ \mathrm{mg\ L^{-1}\ min^{-1}}$). The distinctive loss of TOC was similar to that observed earlier in the photocatalyzed decomposition of 2,4-dichlorophenoxy-acetic acid (2,4-D) [22]. Moreover, as in the dechlorination of 2,4-D, microwave irradiation has relatively little impact on the dechlorination process.

The response of microwave radiation to the photocatalyzed reduction or photo-catalyzed oxidation of reducible and oxidizable substrates (e.g. 4-CP) by electron attachment or attack of $^{\bullet}OH$ radicals, respectively, can originate from either or both thermal and nonthermal factors of the microwave radiation field. Regardless of these effects, however, subjecting aqueous TiO_2 dispersions to microwave radiation alone (no UV) had no effect on the breakup of the aromatic ring of 4-CP, and no impact on the loss of TOC and on the dechlorination of the chlorophenol toxin (see MW data in Fig. 2).

The quantities of carboxylic acids produced in the degradation of 4-CP at various irradiation times are summarized in Table 1 for PD, PD/TH, and PD/MW. The signal with retention time 3.5 min in the HPLC chromatogram (inset to Fig. 2a)

Table 1
Temporal evolution of the formation of carboxylic acid intermediates and benzoquinone during the degradation of 4-CP by the PD, PD/TH and PD/MW methods

	PD			PD/TH			PD/MW		
	30 min	60 min	90 min	30 min	60 min	90 min	30 min	60 min	90 min
Formic acid (mM)	2.6	4.3	4.2	6.4	5.6	0	0	0	0
Acetic acid (mM)	1.3	1.7	6.3	4.4	9.9	28	8.2	19	27
Succinic acid (mM)	3.2	3.0	5.0	4.6	0	3.7	3.3	0	7.7
Benzoquinone (μM)	3.4	1.6	3.4	1.7	5.6	1.9	0	5.9	0

was attributed to the benzoquinone intermediate identified against a standard sample. Other intermediates with other retention times were not identified by the HPLC technique (see Section 2).

Formation of formic acid was confirmed for the PD and PD/TH methods: maximal quantities were ca. 4.3 mM and 6.4 mM, respectively, after 60 min (PD) and 30 min (PD/TH) of irradiation. No formic acid was produced (or at least detected) by the microwave-assisted photocatalytic PD/MW method. Smaller quantities of acetic acid formed through the PD route relative to the larger quantities produced by the PD/TH and PD/MW methodologies after a 90 min illumination period. Formation of succinic acid ($HOOC{-}CH_2{-}CH_2{-}COOH$) was slower in all cases (not shown) requiring irradiation of the dispersion for at least 30 min. Both formic and acetic acid probably resulted from the degradation of succinic acid.

Differences observed in the formation and decay of formic and acetic acids by similar irradiation methods in the degradation of other substrates were earlier attributed to a feature(s) originating with the microwave radiation [20,22,33]. To examine the root of such differences further we determined the dielectric loss coefficient ε'' of formic acid, acetic acid, and water using an Agilent Technologies HP-85070B Network Analyzer. {Note that $\varepsilon'' = \varepsilon' \tan\delta$, where ε' is the specific inductive capacity of the dielectric substance and $\tan\delta$ is the dielectric power factor of the dielectric substance [37]}. The ε'' coefficient of all three above substrates was determined at three different temperatures: 25 °C, 50 °C and 100 °C. The values of ε'' at a microwave frequency of 2.45 GHz decreased in the order: formic acid (27.0) > water (9.58) > acetic acid (1.82) at 25 °C; formic acid (22.7) > water (4.75) > acetic acid (1.87) at 50 °C; and formic acid (13.5) > water (3.85) > acetic acid (1.65) at 100 °C (values interpolated from a frequency of 2.4 GHz and 2.5 GHz). Note that the dielectric loss coefficients refer to the pure substances. Similar considerations of the dielectric loss coefficient were reported earlier [33]. Clearly, the greater dielectric loss coefficient of formic acid, over acetic acid and water, suggests that formic acid absorbed microwave radiation to a greater extent at all three temperatures, thus generating more heat than either H_2O or acetic acid. Consequently, we hypothesize that the absence of formic acid in the PD/MW method has three possible origins: (a) formic acid is not formed during the degradation of 4-CP by the integrated MW/UV irradiation method; (b) formic acid did form as an intermediate in PD/MW, but absorption of a greater amount of microwave radiation may have led to faster degradation through microwave thermal effects – that is, through thermal degradation initiated by microwave caloric heating [38]; (c) the microwave radiation field somehow impacted on the interaction(s) between formic acid and the TiO_2 surface ($^{\bullet}OH$ radicals) to such an extent that it caused formic acid to degrade faster.

Formation and subsequent degradation of the benzoquinone intermediate followed no particular trend with irradiation time for all three methods. The question of benzoquinone is considered in more detail below.

3.2. Probing the microwave nonthermal effect(s) in TiO_2 dispersions

To assess the influence (or lack thereof) of microwave nonthermal (again we emphasize non-caloric) effects on the cleavage of the aromatic ring of 4-CP, on dechlorination, on the loss of TOC, and on the formation of intermediates in the MW-assisted photocatalyzed degradation appropriate experiments were carried out at constant ambient temperature (25 ± 2 °C). For this purpose, we used the microwave oven applicator reported earlier (see the microwave cavity B in Fig. 1 of ref. [33]). This procedure can delineate microwave nonthermal from thermal effects more appropriately without the conventional thermally-assisted influence on the reaction by examining the differences between the PD and PD/MW methods, since the impact of microwave-generated heat on the degradation processes is minimized considerably, if not suppressed at the constant ambient temperature.

In Table 2, we have summarized the quantity of the 4-CP toxin (initially 0.10 mM) remaining in the dispersion (HPLC-UV absorption), formation of intermediates assayed by the HPLC technique during irradiation for 15 and 30 min by the PD_{25} and PD/MW_{25} methods at constant ambient temperature (25 °C), as well as the percent yield of TOC loss and percent dechlorination yield after 30 and 60 min. The HPLC chromatograms displayed only signals for 4-CP, hydroquinone (HQ), benzoquinone (BQ) and catechol (CC), all of which were confirmed from available standards: HQ (RT = 2.5 min), BQ (RT = 3.5 min), and CC (RT = 4.2 min); suitable calibration curves converted the signal amplitudes into concentrations.

Degradation of 4-CP showed only some minor differences between the PD_{25} and PD/MW_{25} methods for similar

Table 2
Summary of 4-CP (0.10 mM) remaining in the TiO_2 dispersion (UV absorption), formation of intermediates assayed by the HPLC technique during irradiation of 4-CP for 15 and 30 min by the PD_{25} and PD/MW_{25} methods at a constant ambient temperature of 25 °C, and the percent yield of TOC loss and percent dechlorination yield after 30 and 60 min irradiation

Substrate/intermediates (λ monitored by HPLC)	PD_{25}		PD/MW_{25}	
	15 min	30 min	15 min	30 min
4-chlorophenol (279 nm)/mM	0.040	0.015	0.037	0
Hydroquinone (288 nm)/μM	–	–	–	9.1
Benzoquinone (245 nm)/μM	15.4	17.1	7.8	36.6
Catechol (274 nm)/μM	19.2	24.4	21.4	18.4

Process	PD_{25}		PD/MW_{25}	
	30 min	60 min	30 min	60 min
% Mineralization (TOC loss)	46	59	42	62
% Dechlorination	70	100	70	100

Light source used was the 250 W Hg lamp; light irradiance, 18 mW cm^{-2}.

irradiation periods, except for the quantity of benzoquinone produced where differences were more significant.

No hydroquinone (HQ) was detected for the PD_{25} method at all irradiation times, whereas the PD/MW_{25} method led to the formation of HQ albeit at the longer irradiation time. For benzoquinone, formation by the PD/MW_{25} method increased rapidly with increasing decomposition time originating from hydroquinone. Catechol was produced by dechlorination of the 4-chlorocatechol (4-CC) intermediate (reaction a1), whereas HQ was likely generated from the dechlorination of 4-CP either by photoreduction (i.e. by electron attachment to the 4-CP substrate) or by oxidation through attack by $^{\bullet}OH$ radicals (reaction a2) in accord with earlier studies [1,5,6]. We deduce that formation of 4-chlorocatechol involved $^{\bullet}OH$ radical addition to the 4-CP positioned near the TiO_2 surface [7], but within reacting distance of the

$$\text{4-CP} + {}^{\bullet}\text{OH} \rightarrow \text{4-chlorocatechol} \rightarrow \text{catechol} \qquad \text{(a1)}$$

$$\text{4-CP} + e^{-}_{cb}(\text{or}\,{}^{\bullet}\text{OH attack; or}\,h^{+}_{vb}) \rightarrow \text{HQ} \rightarrow \text{BQ} \qquad \text{(a2)}$$

$^{\bullet}OH$ radicals on the surface (Scheme 1). Since chemisorption is an exothermic process, microwave-generated (caloric effect) heat lessens chemisorption interactions between the phenolic end of 4-CP and the metal-oxide particle surface. By contrast, in the absence of thermal effects, electron reduction (not shown) and/or attack by $^{\bullet}OH$ radicals at the C–Cl carbon position lead to formation of HQ and to dechlorination of chemisorbed 4-CP [6]. Identification of the precise nature of microwave non-caloric (that is, nonthermal) factors continue to be a challenging task. Nonetheless, they do play a non-insignificant role.

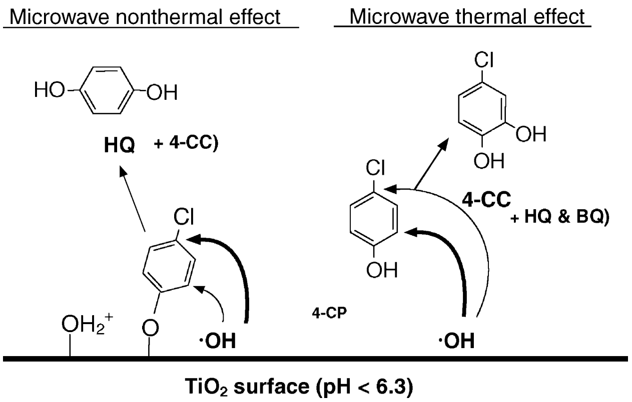

Scheme 1. Proposed mechanism of the role of microwave nonthermal effect versus thermal effect in the formation of hydroquinone (HQ) and 4-chlorocatechol (4-CC) by the PD/MW_{25} method in aqueous TiO_2 dispersions.

The slight difference (ca. 3–4%; Table 2) in the extent of mineralization between the PD_{25} and the PD/MW_{25} methods may be due to slight variations in the dynamics of decomposition of the photogenerated intermediates. By contrast, microwave effects (thermal and nonthermal) have no role in the dechlorination process under these conditions. Despite the small magnitude of the microwave effects witnessed in the data of Table 2, the non-caloric factors of the microwave radiation field can influence the degradation of intermediates and thus the overall decomposition of the chlorophenol toxin.

3.3. Detection and identification of intermediates by the ESI–MS mass spectral method

Detection and identification of intermediates produced in the degradation of 4-CP were carried out by electrospray mass spectral techniques by both the positive-ion (pos: $M + H^+$ or $M + Na^+$) and negative-ion (neg: $M - H^+$) modes. The mass numbers m/z of species formed are listed in Table 3. The initial 4-CP substrate was seen at $m/z = 127$ and 129 in the negative-ion mode {two peaks consistent with a substance bearing a chlorine substituent; mass ratio of the two Cl isotopes is 100:32} as ascertained from standards database of the LC–MSD manufacturer (Agilent Technologies). Several LC-MS spectral intermediates were produced (Fig. 3) by the PD, PD/TH and PD/MW methods after 60 min of irradiation. To emphasize the smaller peaks, the peak at $m/z = 127$ (4-CP) was deleted from the mass spectra. The negative-ion mode signals at $m/z = 93$, 109, 123, 125 and 143 are, respectively, those of phenol, hydroquinone (HQ) or

Table 3
Positive and negative ion ESI mass spectral numbers in the decomposition of 4-CP after 30, 60 and 120 min of irradiation by the PD, PD/TH and PD/MW routes

	PD		PD/TH		PD/MW	
	Positive (*m*/*z*)	Negative (*m*/*z*)	Positive (*m*/*z*)	Negative (*m*/*z*)	Positive (*m*/*z*)	Negative (*m*/*z*)
30 min	–	93, 109, 123, 125, 127/129 (Cl), 173	–	93, 109, 117, 123, 127/129 (Cl), 143, 163, 173	143	59, 93, 127/129 (Cl)
60 min	143	93, 117, 123, 127/129 (Cl), 143 (Cl)	145 (Cl) 199 (Na)	93, 127/129 (Cl), 143, 163, 173, 254/256/258 (2Cl)	143	103, 109, 127/129 (Cl), 163, 254/256/258 (2Cl)
120 min	–	103, 109, 125, 127/129 (Cl), 143 (Cl), 173	145 (Cl)	59, 93, 109, 117, 123, 127/129 (Cl), 143, 173	223 (Na)	59, 93, 103, 109, 117, 127/129 (Cl), 143, 143/145 (Cl), 157, 254/256/258 (2Cl)

(Cl) indicates a substance having one chlorine substituent, whereas 2Cl indicates a substance with two chlorine functions; (pos): positive ion mode; (neg): negative ion mode. Light source used was the 75 W Hg lamp; light irradiance, 0.3 mW cm^{-2}.

catechol, hydrobenzoquinone (HBQ), hydroxyhydroquinone (HHQ), and 4-chlorocatechol (4-CC); the signals at *m*/*z* = 223 (positive) and 254 (negative) belong to the intermediates 4-hydroxyphenylbenzoquinone and 2-(4′-chlorophenyl)-4-chlorocatechol.

Bahnemann and coworkers [1] previously reported generation of these intermediates in aqueous alkaline media (pH > 7). Our current results show these substances to be formed by the PD/MW route in acidic media at pH < 7 (initial pH of 4-CP solution was 6.0), albeit under different

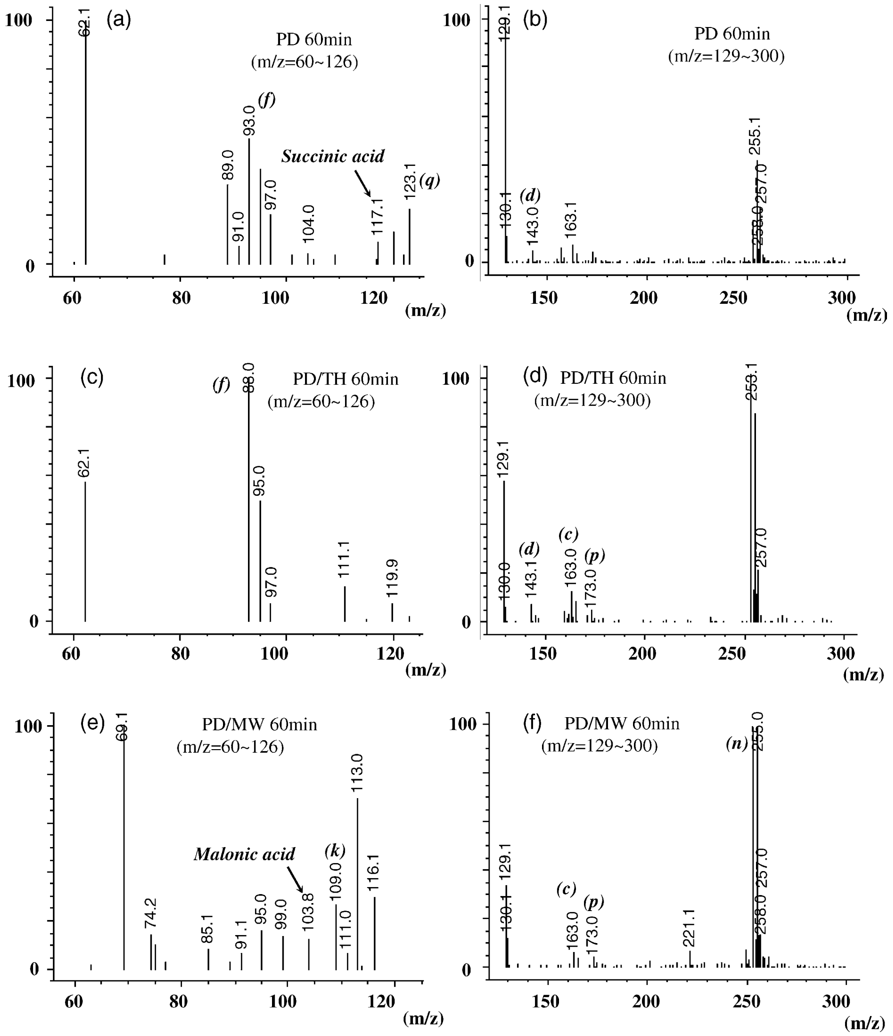

Fig. 3. Electrospray mass spectra (negative-ion mode) recorded during the decomposition of 4-CP by the PD, PD/TH and PD/MW methods after 60 min of irradiation. The peak at *m*/*z* = 127 (4-CP) was removed in order to emphasize the weaker peaks.

experimental conditions. The above results suggest various primary degradative mechanistic steps for the degradation of 4-chlorophenol that we examine below.

3.4. Nature of the intermediates and proposed degradation mechanisms

Comparison of the intermediates detected in the microwave-assisted photocatalytic degadation of 4-CP from those obtained from the photocatalytic method alone is rather instructive [1–3]. The various intermediates produced from the PD/MW, PD/TH, and PD methods and possible relevant steps are summarized in Scheme 2a–c, respectively.

For the PD/MW irradiation method, four initial elementary channels are postulated on the basis of the data of Table 3 and Fig. 3. Channel 1 involves attack of the •OH radical on the C–Cl carbon position to yield the radical intermediate (***a***), followed by dechlorination to give the HQ(***g***)/BQ(***h***) species, and the cyclic propoxide intermediate (***b***), which hydrolyzes to the ring-opened species (***c***). Continued hydrolysis of (***c***) yields intermediates (***d***) and (***e***) followed by further degradation to give succinic acid, malonic acid (identified by HPLC) and acetic acid (note: no formic acid was detected – see above discussion) on their way to CO_2. Channel 2 involves electron reduction of 4-CP to yield phenol (***f***). Hydrolysis of the precursor hydroxylphenyl radical also leads to HQ (***g***) and BQ (***h***), which on continued hydroxylation by •OH radicals forms the inferred (but not detected by the ESI–MS method) HBQ and HHQ intermediates followed by ring opening (intermediate ***o***) and subsequent formation of the carboxylic acid species. Channel 3 is thought to involve addition of •OH to 4-CP to produce 4-chlorocatechol (***i***), which upon dechlo-

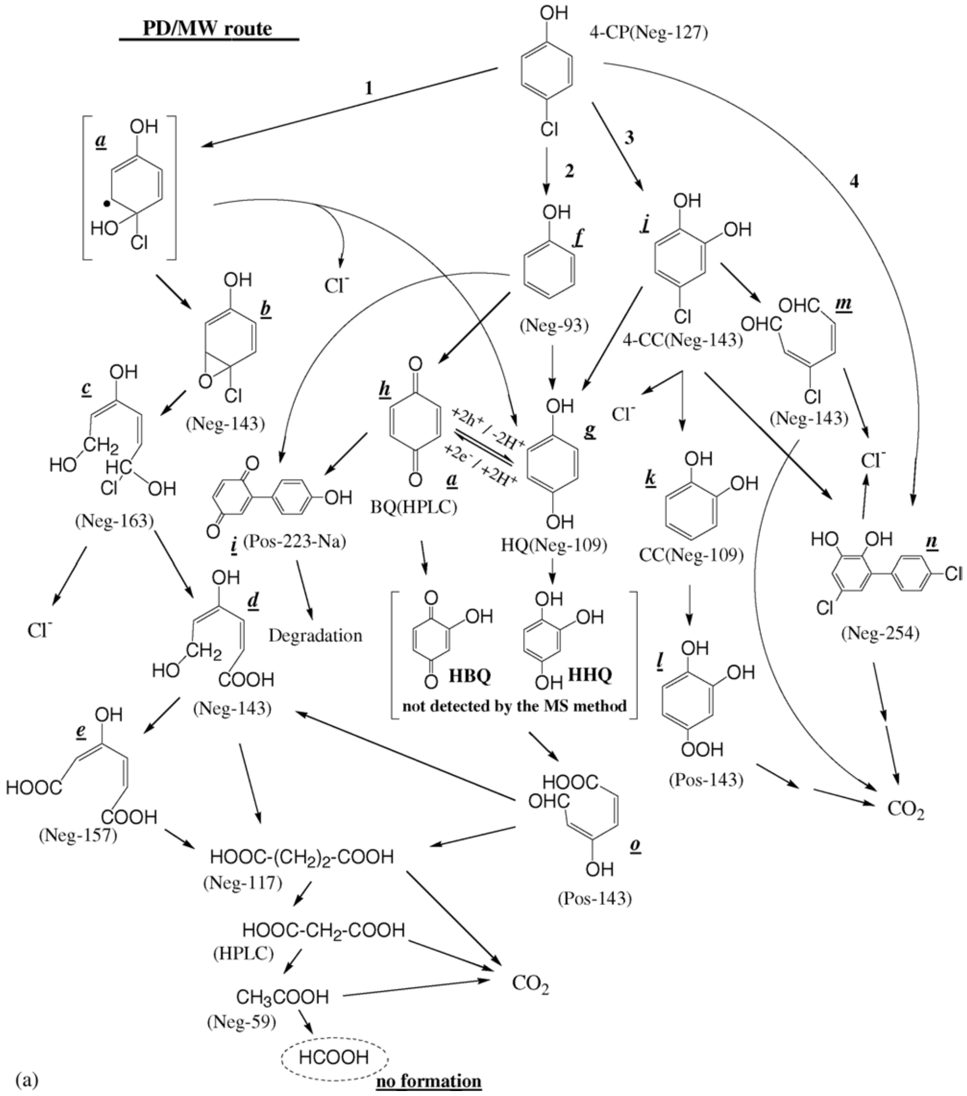

Scheme 2. (a) Gross overview of some of the mechanistic steps based on intermediates identified by the ESI–MS technique in the degradation of 4-CP by the PD/MW method. (b) Gross overview of some of the mechanistic steps based on intermediates identified by the ESI-MS technique in the degradation of 4-CP by the PD/TH method. (c) Gross overview of some of the mechanistic steps based on intermediates identified by the ESI–MS technique in the degradation of 4-CP by the PD method.

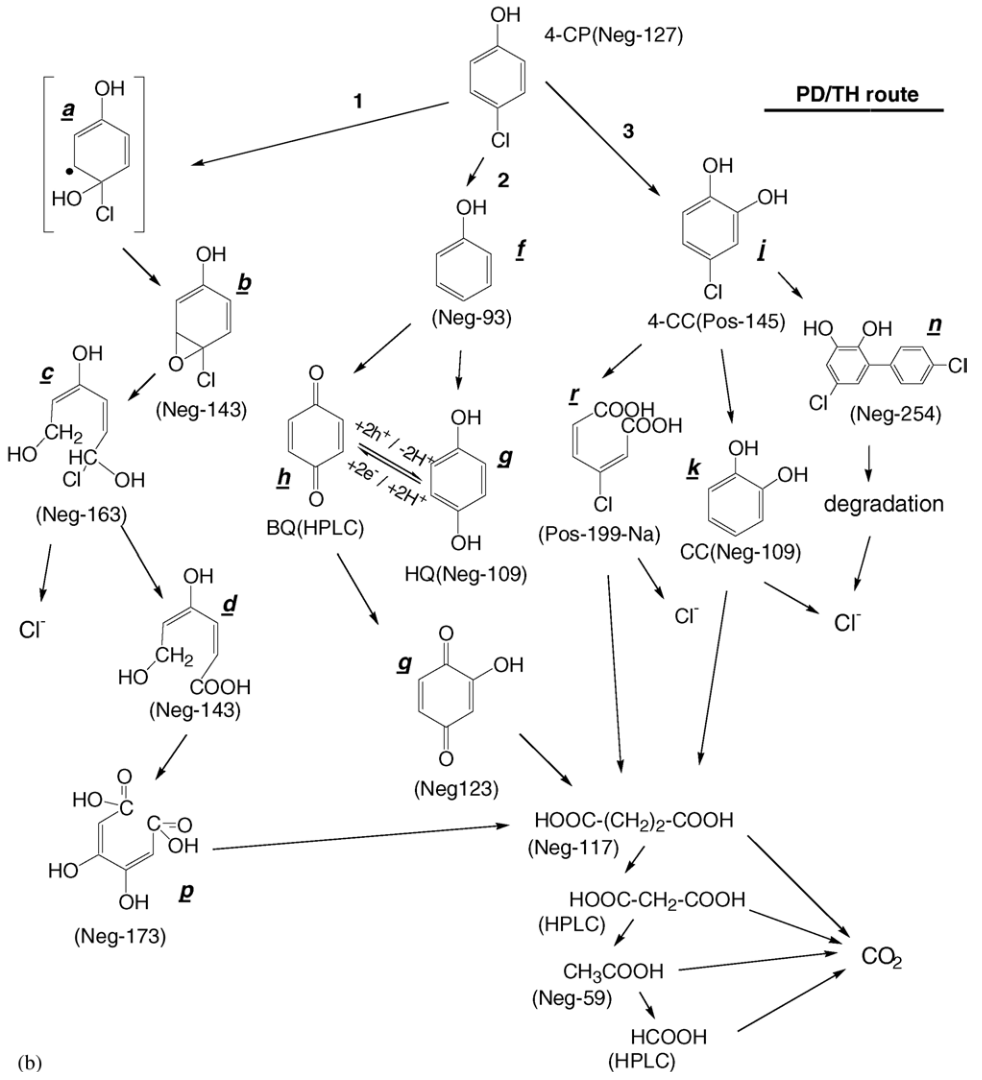

Scheme 2. (*Continued*)

rination yields catechol (***k***) followed by species (***l***) and (***o***), as well as intermediates (***m***) and (***n***). The last channel (step 4) suggests that the dichlorodihydroxybiphenyl intermediate (***n***) forms from reaction between 4-chlorophenol and 4-chlorocatechol.

Peculiar hydrolytic features are inferred in the degradation of 4-CP when using the PD/TH (path 1 in Scheme 2b) and the PD/MW method (channel 1 in Scheme 2a) that were not seen in the PD method (Scheme 2c). The thermal effect, whether from conventional or microwave-generated heat, was responsible in part for the formation of intermediates (***b***) and (***c***) – no equivalent was discerned in the photocatalytic (PD) method alone. For path 2 (Scheme 2b), the HQ (***g***) intermediate is formed subsequent to formation of phenol (intermediate ***f***) through a photoreductive path involving the hydroxyphenyl radical precursor. Formation of BQ, observed by HPLC (RT = 3.5 min; inset in Fig. 2a), originates from HQ. Formation of BQ and the hydroxyphenyl radical by the PD/MW and PD/TH methods (channel 2 in Scheme 2a and b) explains the formation of the 4-hydroxyphenylbenzo-quinone intermediate (***i***) seen by the PD/MW method in Scheme 2a but not by the thermally-assisted PD/TH method (Scheme 2b), nor by the photocatalytic PD method alone (Scheme 2c).

In the TiO_2-photocatalyzed degradation, BQ and HQ are mineralized by further irradiation through intermediates HBQ {***q***; *m*/*z* = 123 (neg); Scheme 2b} and HBQ and HHQ {***q*** and ***s***; *m*/*z* = 123 (neg) and 125 (neg); Scheme 2c}. Curiously, the PD/MW method failed to produce these two intermediates ***q*** and ***s***. We infer that either the microwave radiation affected their formation, or else the microwave nonthermal factors increased the rate of secondary reactions (ring opening) such that they went undetected. Note that in the thermally-assisted PD/TH method, intermediates HBQ and HHQ were detected (Scheme 2b) inferring that microwave-generated heat (thermal effect) played no role for their absence in the PD/MW method.

Formation of 4-CC (intermediate ***j***) takes place through previous formation of the adduct between 4-CP and the

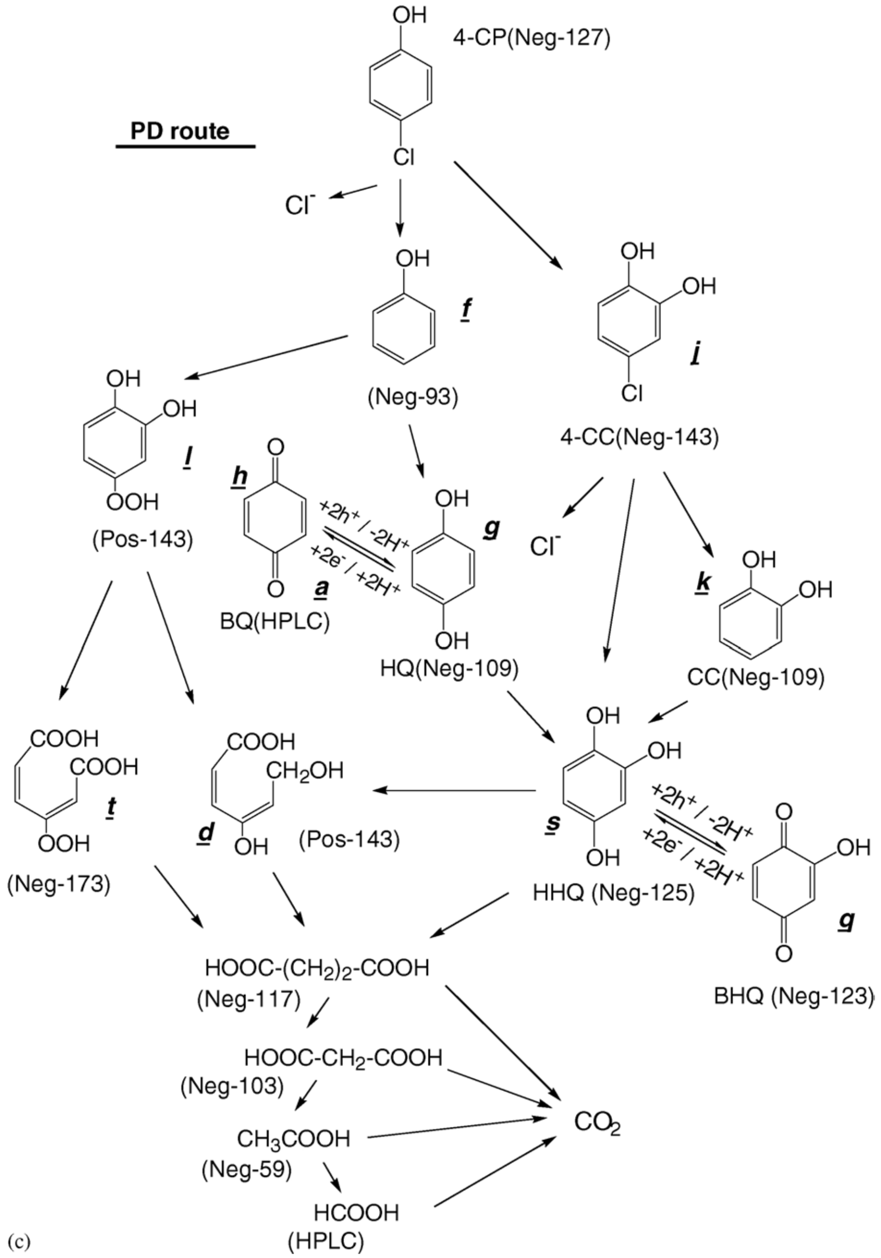

Scheme 2. (*Continued*).

$^\bullet$OH radicals in all three methods examined. Dechlorination of 4-CC yields catechol (intermediate ***k***) which subsequent to ring opening leads to succinic, malonic, acetic, and formic acids, and ultimately to complete mineralization to CO_2 through both PD/TH and PD. In channel 4 of Scheme 2a and path 3 of Scheme 2b, intermediate ***n*** {2-(4′-chlorophenyl)-4-chlorocatechol} can also originate from reaction(s) between two 4-CP molecules or between 4-CP and 4-CC. Clearly, with minor exceptions, the same intermediates formed, whether by conventional thermally-assisted photocatalytic degradation or by a photocatalytic reaction subjected to a microwave radiation field. The major difference between the PD/MW and the PD/TH methods lies in the apparent absence of HBQ and HHQ species. Moreover, the intermediates 4-hydroxyphenylbenzoquinone and 2(4′-chlorophenyl)-4-chlorocatechol, originally detected in TiO_2 dispersions in alkaline solution [1], were also produced by the PD/MW method.

3.5. Photodegradation of hydroqinone (HQ) in TiO_2 dispersions

Since hydroquinone was an important intermediate in the degradation of 4-CP, an original sample of HQ was also subjected to the three photocatalytic methods to assess the fate of HQ under these conditions, and perhaps provide addi-

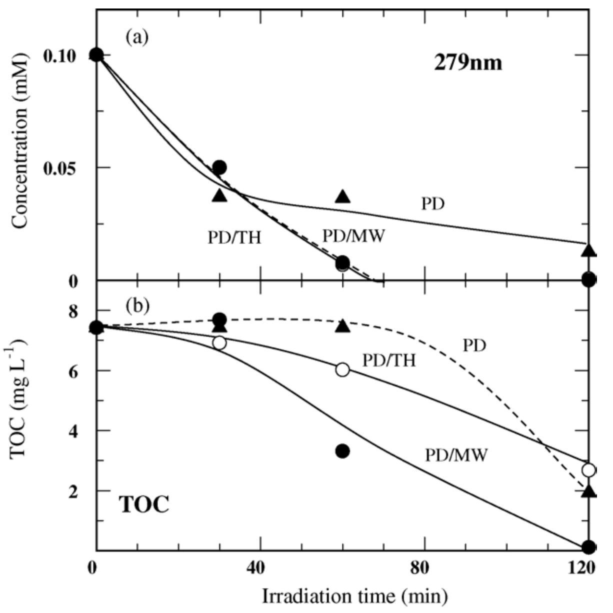

Fig. 4. (a) Time profiles of the degradation of hydroquinone (HQ) using loss of UV absorption in the HPLC chromatogram, and (b) of the loss of total organic carbon (TOC) in the decomposition of HQ (0.1 mM) in aqueous media by photocatalyzed oxidation (PD), thermally-assisted photocatalyzed oxidation (PD/TH) and by the integrated microwave-assisted photocatalyzed degradation (PD/MW) using a 250 W mercury lamp to provide the UV radiation.

tional details to an otherwise complex pathway. The temporal decrease of UV absorption in the HPLC chromatogram of HQ (RT = 2.5 min) in the photocatalyzed degradation of hydroquinone is illustrated in Fig. 4a. Irradiation was carried out using the Ushio 250 W mercury lamp since degradation of HQ tended to be rather slow with the 75 W light source. The extent of degradation of HQ followed the order PD/TH (93%) ≈ PD/MW (92%) > PD (63%) after 60 min of irradiation with the PD/MW and PD/TH methods displaying nearly identical temporal profiles. By contrast, loss of TOC (Fig. 4b) was greatly influenced by the method chosen to degrade HQ.

The initial quantity of TOC (7.35 mg L^{-1}; 0.10 mM) decreased to 0 mg L^{-1} for the PD/MW method (100% loss), and dropped to 2.0 mg L^{-1} for PD (ca. 73% loss) and to 2.8 mg L^{-1} for the PD/TH method (ca. 62% loss) on irradiation for 120 min. The variations observed in Fig. 4b suggest that, subsequent to total cleavage of the HQ aromatic ring, conventional and microwave-generated thermal effects promoted further degradation of the intermediates as compared to the PD method. Moreover, it is also evident that non-caloric (nonthermal) microwave factors also play a role: compare for example the PD/MW and PD/TH data in Fig. 4b.

Formation of hydroxyhydroquinone (HHQ) was probed by the mass spectral technique (negative-ion mode) for all three PD, PD/TH and PD/MW methods. The mass peak at $m/z = 125$ (neg) in the PD method seen after 120 min of irradiation is that of the HHQ intermediate, which was not detected in the PD/TH and PD/MW methods. This infers that HQ must undergo very fast degradation through ring cleavage to ultimate mineralization by the latter two methods, in accord with the notions summarized in Scheme 2a and b.

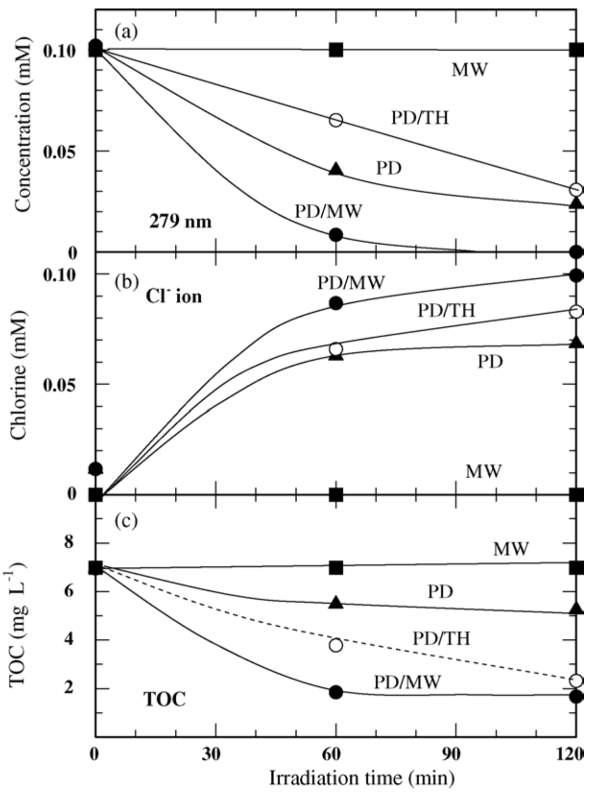

Fig. 5. Time profiles of the degradation of 4-CP (loss of UV absorption in the HPLC chromatogram) (a), of the formation of Cl^- ions (b), and of the loss of TOC in the degradation of 4-CP by the MW, PD, PD/TH and PD/MW irradiation of aqueous Pt/TiO_2 dispersions.

3.6. Photocatalyzed degradation of 4-CP in platinized TiO_2 dispersions

Fig. 5 compares the results of the degradative process for 4-CP taking place through the PD, PD/TH and PD/MW methods in Pt/TiO_2 dispersions and monitored (a) by loss of UV absorption at 279 nm in the HPLC chromatogram; (b) by dechlorination; and (c) by loss of TOC. The most significant difference with naked TiO_2 dispersions (see Fig. 2) is the relatively faster degradation of 4-CP by the PD/MW and PD methods. The kinetic data of Table 4 indicate that degradation of 4-CP followed the order PD/MW > PD > PD/TH, paralleling the trend in naked TiO_2 dispersions. Evidently, conventional heating of the photocatalytic process (PD/TH) is the least effective in ring opening of the 4-CP structure.

The greater acceleration of the process by the Pt cocatalyst on the TiO_2 surface through PD/MW, relative to PD/TH, must implicate nonthermal factors of the microwave radiation field. Photomineralization of 4-chlorophenol (TOC loss) through the microwave-assisted photocatalytic process is favored over the conventionally heated PD/TH method; relevant ratios are PD/MW:PD:PD/TH = 3:2:1. By contrast, photomineralization of 4-CP on naked TiO_2 parti-

Table 4
Approximate kinetics (k) in the degradation of 4-CP for 120 min of irradiation by the PD, PD/TH and PD/MW methods in naked TiO_2 (P-25) and Pt/TiO_2 dispersions

	Kinetics of degradation of 4-CP and of TOC loss		Kinetics of dechlorination
	$k_{degradation}$ (min^{-1})	k_{TOC} (min^{-1})	k_{Cl^-} (min^{-1})
TiO_2			
(PD)	0.01 (1)[a]	0.005	0.025
(PD/TH)	0.01 (1)	0.005	0.025
(PD/MW)	0.02 (2)	0.005	0.025
Pt/TiO_2			
(PD)	0.02 (3)	0.02 (2)	0.030
(PD/TH)	0.006 (1)	0.01 (1)	0.025
(PD/MW)	0.03 (5)	0.03 (3)	0.025

[a] Normalized ratios to the PD/TH value.

Table 5
Percent degradation, mineralization (TOC loss) and dechlorination during the degradation of 4-CP in naked TiO_2 and Pt/TiO_2 aqueous dispersions after 120 min of irradiation by the PD, PD/TH and PD/MW methods

System	Percent degradation	Percent mineralization	Percent dechlorination
TiO_2 (PD)	65	60	87
(PD/TH)	55	36	87
(PD/MW)	90	60	100
Pt/TiO_2 (PD)	76	26	68
(PD/TH)	70	66	83
(PD/MW)	100	77	100

cles (Table 4) seems indifferent on whether the photoprocess is microwave-assisted or thermally-assisted. In comparison, dechlorination of 4-CP occurred under otherwise identical kinetics (within experimental error) indicating that platinization of titania had no particular effect on the kinetics of dechlorination.

Table 5 compares the extent (in %) of degradation, mineralization, and dechlorination of 4-CP in naked TiO_2 and Pt/TiO_2 aqueous dispersions after a 120 min irradiation period. Clearly, platinization of the titania photocatalyst led to greater degradation (100% by the PD/MW method) and to greater mineralization of 4-CP than was the case for naked TiO_2 photocatalyic processes. By contrast, platinization was rather inconsequential on the extent of dechlorination of 4-CP. In fact, platinization of TiO_2 was less efficient in the dechlorination by the PD method than was otherwise the case for naked TiO_2 alone. Similar observations are evident in the mineralization of 4-CP, whereby naked TiO_2 appears advantageous in the evolution of CO_2 (i.e. decaying TOC). Differences between the three photocatalytic methods caused by the presence of the Pt co-catalyst on the TiO_2 surface, accompanied by irradiation with microwaves, are most prominent in the degradation of the intermediates produced (Table 6). The degradation of 4-CP produced three intermediates within 120 min of irradiation by the PD method, identified by HPLC as HQ, BQ and catechol (CC). The PD/TH method led to formation of BQ and CC, whereas only BQ was seen after 60 min of irradiation by the PD/MW method indicating that this method leads rapidly to further degradation of the intermediates. Thus, the most suitable method of degradation of 4-CP is clearly the PD/MW method using platinized-TiO_2 photocatalysis.

3.7. Probing the microwave thermal and nonthermal effect(s) in Pt/TiO₂ dispersions

The relevance of microwave-generated caloric (thermal) effects against microwave nonthermal effects was examined for the photodegradation of 4-CP under ambient constant temperature (25 °C) by comparing the photocatalyzed process (PD method) against the microwave-assisted PD/MW method. Maintaining the temperature constant shows whether thermal or nonthermal (or both) microwave effects influence the decomposition of the chlorophenol toxin. The experimental conditions were otherwise identical to those used to obtain the results summarized in Table 2.

Both degradation and mineralization (Table 7) were not affected when microwave irradiation was coupled to UV illumination of the Pt/TiO_2 photocatalyst. This infers that the thermal component of the microwave radiation field is highly relevant to these two processes and explains the results illustrated in Fig. 5 (see also Table 5). By contrast, dechlorination of 4-CP was more effective after 30 min of irradiation by the PD/MW relative to PD photocatalysis at constant temperature demonstrating that dechlorination is to some extent influenced by nonthermal effects of the microwave radiation. This contrasts the results obtained in the degradation of 4-CP carried out in naked TiO_2 dispersions (Table 2), whereby the nonthermal component of the microwave radiation field played no role in the dechlorination process.

Table 6
Summary of formation of intermediates detected by the HPLC technique during the irradiation of 4-CP for 60 and 120 min, in the presence of the Pt/TiO_2 photocatalyst at the indicated monitoring wavelengths

	PD		PD/TH		PD/MW	
	60 min	120 min	60 min	120 min	60 min	120 min
Hydroquinone (288 nm)/μM	0.011	0.0080	0.00050	nd[a]	nd	nd
Benzoquinone (245 nm)/μM	0.31	0.37	0.064	0.047	0.014	nd
Catechol (274 nm)/μM	0.011	0.013	0.012	0.010	nd	nd

[a] None was detected.

Table 7
Degradation, loss of TOC, formation of Cl^- ions and the intermediates 4-CC, HQ and BQ in the mineralization of 4-CP by the PD_{25} and PD/MW_{25} methods with Pt/TiO_2 photocatalysis at constant ambient temperature (25 °C). Light source used for irradiation was the 250 W Hg lamp; light irradiance, 18 mW cm^{-2}

Process	PD_{25}		PD/MW_{25}	
	15 min	30 min	15 min	30 min
% Degradation (HPLC; 279 nm)	81	78	79	82
% Mineralization	52	96	48	96
% Dechlorination	86	86	90	100
Intermediates				
4-Chlorocatechol (283 nm)/μM	0.017	0.024	0.011	0.011
Hydroquinone (288 nm)/μM	0.016	0.008	0.009	0.010
Benzoquinone (245 nm)/μM	0.170	0.019	0.380	0.270

Degradation of 4-CP occurring either by oxidative attack of $^{\bullet}OH$ radicals or by the photoreductive path through photogenerated electrons trapped on the Pt co-catalyst led to formation of three intermediates [5,6] on naked TiO_2 albeit under different conditions. Formation of 4-CC is governed by attack of $^{\bullet}OH$ radicals, whereas both a photooxidative (through hydroquinone) and photoreductive path can lead to formation of BQ. Formation of HQ can also involve both pathways, either through $^{\bullet}OH$-radical displacement of the 4-chloro substituent or through hydrolysis of the hydroxyphenyl radical ($^{\bullet}OH$ radicals or H_2O). The greater quantity of BQ produced by the PD/MW method (Table 7) is due to photoreduction of the chlorophenol [6] on the UV-irradiated Pt/TiO_2 under a microwave radiation field. The data also demonstrate that thermal effects bear significantly on the cleavage of the benzene ring, contrasting our earlier findings with other substrates [21,23,33]. In the present instance, nonthermal factors have their greatest influence on dechlorination. A role of both thermal and nonthermal factors is also evident in the generation and decay of the type of intermediates produced.

3.8. Oxidative radicals

A key factor that affects the efficient photodegradation of organic pollutants using TiO_2 photocatalysis is the dependence on the concentration of oxidizing radicals. Titania particles (anatase) absorb UV light at energies greater than 3.10 eV for naked TiO_2 and > 3.11 eV for Pt/TiO_2 to generate electron/hole pairs (reaction b1). Valence band holes (h_{vb}^+) are subsequently trapped by surface-bound HO^- ions (or by sorbed H_2O) to yield $^{\bullet}OH$ radicals (and H^+; reaction b2). Concomitantly, the conduction band electrons (e_{vb}^-) are scavenged by adsorbed O_2 molecules to yield superoxide radical anions, $O_2^{-\bullet}$, in competition with surface Ti^{4+} ions to give the corresponding Ti^{3+} trapped-electron surface states. Protonation of $O_2^{-\bullet}$ yields $^{\bullet}OOH$ radicals (reactions b3 and b4). Recombination of trapped electrons in the superoxide radical anions with h_{vb}^+ yields singlet oxygen ($^1O_2$) [39], also a powerful reactive oxygen species, which cannot be precluded in oxidations although its precise role remains a matter of further study. Accordingly, we consider photooxidation of 4-CP to take place through either $^{\bullet}OH$ and/or $^{\bullet}OOH$ radical attack on the positions of highest electron density in the 4-CP molecules (reaction b5). For Pt/TiO_2, conduction band electrons (e_{cb}^-) trapped on the Pt co-catalyst accentuate the reduction of oxygen molecules (reaction b7) in competition with

$$TiO_2 + h\nu_{\lambda<388nm} \rightarrow TiO_2(e_{cb}^- + h_{vb}^+) \quad (b1)$$

$$h_{vb}^+ + OH^-(H_2O) \rightarrow {}^{\bullet}OH(H^+) \quad (b2)$$

$$e_{cb}^- + O_2 \rightarrow O_2^{-\bullet} \quad (b3)$$

$$O_2^{-\bullet} + H^+ \rightarrow {}^{-\bullet}OOH \quad (b4)$$

$$\begin{aligned}&{}^{\bullet}OH\,(\text{or}\ {}^{\bullet}OOH) + \text{4-CP} \rightarrow \text{Intermediates}\\ &\quad\rightarrow CO_2 + H_2O + Cl^- \quad (b5)\end{aligned}$$

$$h_{vb}^+ + \text{4-CP} \rightarrow \text{4-CP}^{+\bullet} \rightarrow\rightarrow CO_2 + H_2O + Cl^- \quad (b6)$$

$$e_{cb}^- + \frac{Pt}{TiO_2} \rightarrow \frac{Pt^-}{TiO_2} \xrightarrow{O_2} O_2^{-\bullet} \quad (b7)$$

$$\begin{aligned}&e_{cb}^- + \frac{Pt}{TiO_2} \rightarrow \frac{Pt^-}{TiO_2}\\ &\quad\xrightarrow{4-CP} \text{Dechlorinated intermediates and products} \quad (b8)\end{aligned}$$

dechlorination of 4-CP (reaction b8). Note that the direct initial photodegradation of 4-CP by h_{vb}^+ (stage b6) on the TiO_2 surface, though not precluded by our present data, is deemed unlikely [40].

Formation of $^{\bullet}OH$ and $^{\bullet}OOH$ radicals during TiO_2-photocatalyzed oxidations driven by simultaneous UV and microwave radiation was probed by electron spin resonance techniques employing a novel set-up in which the EPR sample (contained the DMPO spin-trap agent and naked TiO_2 or Pt/TiO_2 in aqueous media) could be irradiated by both UV light and microwaves. The output power of the microwave radiation was ca. 2 W incident on the sample in the planar quartz cell located in the EPR cavity. The UV irradiation source was an Ushio 250 W mercury lamp whose UV light irradiated the sample from a diagonally lower position of the sample through a fiber optic light-guide. Air-equilibrated aqueous dispersions (2.5 mL; pH 5.8) containing TiO_2 and Pt/TiO_2 particles (loading, 5 mg) and the DMPO spin-trap (5,5-dimethyl-1-pyrrolidine-*N*-oxide; 50 μL) were sonicated for ca. 30 s in the dark, and then introduced into the sample planar cell also under dark conditions, subsequent to which irradiations and scanning the spectra were initiated simultaneously. Other features of the microwave/UV set-up and the EPR system were reported previously [34]. The EPR spectral peak intensities were obtained automatically relative to a standard Mn^{2+} marker using the appropriate software of the JEOL JESTE200 ESR spectrometer. The ratios reported in the in the EPR spectra (Fig. 6) of the DMPO$-{}^{\bullet}$OH and

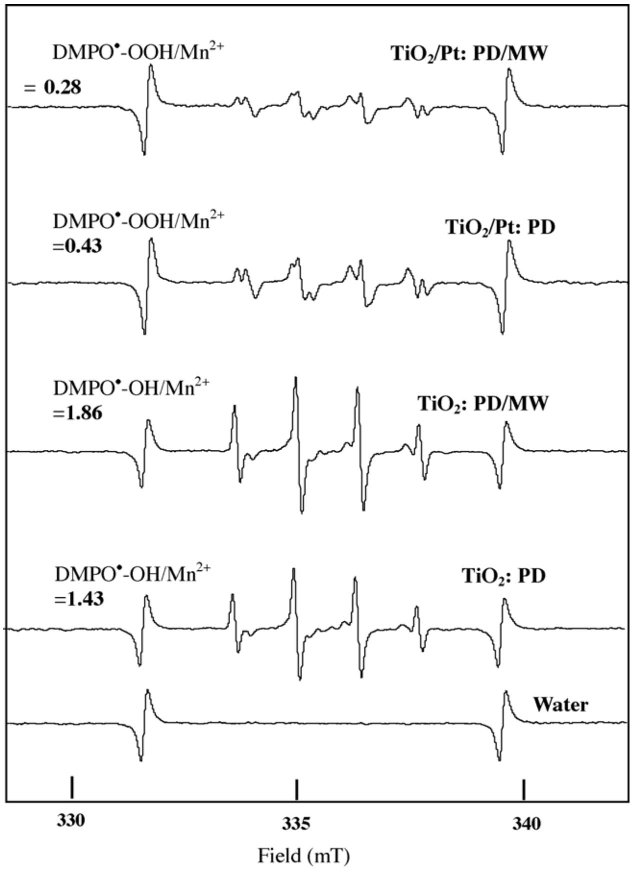

Fig. 6. ESR spectral features of the DMPO–•OH and DMPO–•OOH spin-adducts formed upon irradiation of water alone, aqueous TiO_2 dispersions, and Pt/TiO_2 aqueous dispersions by UV light alone (PD method) and by the combined UV light and MW radiation (UV/MW method).

DMPO–•OOH spin-adducts produced in the various TiO_2 and Pt/TiO_2 heterogeneous systems under UV irradiation, and/or coupled MW/UV irradiation, represent values corrected for the small number of radicals produced on sonication.

The naked TiO_2 system displayed the classical though slightly non-symmetrical 1:2:2:1 spectral signature of DMPO spin-trapped •OH radicals. The lack of symmetry in the four-line ESR signature of DMPO–•OH adducts may be caused either by variations in the environmental microviscosity about the spin probe or by changes in the interactions of the spin probe with the TiO_2 particle surface [41]. The platinized TiO_2 system displayed mixed signals for the DMPO spin-trapped •OH and •OOH radicals in accord with previous observations by Noda and coworkers [42]. The number of •OH radicals produced on naked TiO_2 by the PD/MW method was nearly 30% greater than by the PD method, whereas, smaller quantities of •OOH and •OH radicals were produced on irradiated Pt/TiO_2 by the PD/MW method. We attribute the decrease in the number of these oxygen radicals accompanying microwave irradiation to the photoreduction of oxygen and its subsequent binding to platinum from microwave-generated heating the Pt co-catalyst. However, in the presence of another reducible substrate, such as 4-CP, the trapped electrons on platinum favor reduction of this reducible chlorophenol to produce BQ [6] at the expense of oxygen reduction, as evidenced from the data reported in Table 7 for the PD/MW_{25} method involving the Pt/TiO_2 system.

3.9. *The nature of microwave nonthermal effects in photocatalysis*

Microwave nonthermal effects implicated in the overall degradation of 4-chlorophenol were also considered earlier in relation to the photodecomposition of other substrates [21,22]. To obtain further information on the nature of these nonthermal factors, we assessed the dielectric loss coefficient ε'' of naked TiO_2 and Pt/TiO_2 pellets, prepared using a press operated under high pressures (ca. 1000 kg cm^{-2}) so as to eliminate air between the particles as ε'' is dependent upon the form of the substrate being examined. Note that the crystalline structure of the photocatalyst in pellet form is not modified under high pressures. The measured dielectric loss coefficient of naked TiO_2 was $\varepsilon'' = 0.20$; for the platinized titania, Pt/TiO_2, pellet $\varepsilon'' = 0.29$ at a microwave frequency of 2.45 GHz. The level of microwave radiation absorbed by TiO_2 and Pt/TiO_2 powders (800 mg) under dark conditions was monitored by temperature increase of the two specimens.

The TiO_2 particles had previously been treated at 145 °C in an electric furnace for ca. 30 min; this heat treatment did not remove the ubiquitous chemisorbed water present on the TiO_2 surface. Initially at 25 °C, each sample reached ca. 100 °C after being microwave-irradiated for about 183 s (naked TiO_2) and 135 s (Pt/TiO_2), with the rate of increase of temperature being, respectively, 0.41 °C s^{-1} and 0.56 °C s^{-1}. The Pt co-catalyst in the Pt/TiO_2 sample was inductively heated, acting subsequently as a heat conductor, making induction heating of Pt/TiO_2 particles occur faster than for naked TiO_2 particles.

Formation of localized hot micro-/nano-scale domains, so-called “hot spots”, on the TiO_2 surface by microwave irradiation, or selective heating of photocatalytic active sites on the photocatalyst may also lead to microwave effects similar to those attributed to microwave nonthermal factors. We presume that such localized hot domains have plasma-like properties in certain parts of the TiO_2 surface. Various workers have invoked the role of hot spots in chemical reactions occurring under a microwave radiation field [43–47]. Tsai et al. [48] emphasized the role of hot spots in their electrochemical studies with Pt electrodes. Unfortunately, the temperature of these hot spots over such a small fraction of the TiO_2 particle surface cannot be estimated. In addition, the platinum deposits on the TiO_2 surface may also generate polarized domains on the metal-oxide particle surface under the microwave radiation field. Consequently, the degradation of 4-CP through the PD/MW method may be enhanced when occurring at or near hot localized domains or polarized domains. Enhancement of metal-support-interactions between the Pt deposits and the metal-oxide surface by the microwave radiation field can also modify the activity of the Pt co-catalyst on the support. It would also not be unlikely for the microwave radiation field to restructure the metal-oxide particle surface so as to increase the number of catalytically active sites. Certainly, the greater number of •OH radicals produced in naked TiO_2 specimens attests to the role that microwave nonthermal factors may have in photocatalysis.

Regardless, whatever the precise origin/nature of microwave nonthermal factors, they nonetheless do cause changes to occur in the overall degradative process that cannot be ascribed to simple conventional heating or microwave-generated heating of the dispersions.

Acknowledgments

We greatly appreciate the financial support from the Frontier Research Promotion Foundation as well as a Grant-in-Aid for Scientific Research no. 1450544 (to H.H.) of the Japanese Ministry of Education, Culture, Sports, Science and Technology, and from the Ministero dell'Istruzione, Universita e Ricerca (MIUR, Roma to N.S.). We also wish to express our sincere thanks to the personnel of Hitachi Display Devices, Ltd. and Shikoku Keisoku Instrument Co. Ltd. for their valuable technical support.

References

[1] J. Theurich, M. Lindner, D.W. Bahnemann, Langmuir 12 (1996) 6368.
[2] X. Li, J.W. Cubbage, T.A. Tetzlaff, W.S. Jenks, J. Org. Chem. 64 (1999) 8509.
[3] X. Li, J.W. Cubbage, W.S. Jenks, J. Org. Chem. 64 (1999) 8525.
[4] K.A. Gray, U. Stafford, Res. Chem. Intermed. 8 (1994) 835.
[5] A.V. Emeline, A. Salinaro, N. Serpone, J. Phys. Chem. B 104 (2000) 11202.
[6] A.V. Emeline, N. Serpone, J. Phys. Chem. B 106 (2002) 12221.
[7] U. Stafford, K.A. Gray, P.V. Kamat, J. Phys. Chem. 98 (1994) 6343.
[8] R.W. Matthews, Water Res. 24 (1990) 653.
[9] A. Hiskia, A. Mylonas, E. Papaconstantinou, Chem. Soc. Rev. 30 (2001) 62.
[10] J.-C. D'Oliveira, C. Minero, E. Pelizzetti, P. Pichat, J. Photochem. Photobiol. A:Chem. 72 (1993) 261.
[11] P. Boule, C. Guyon, J. Lemaire, Toxicol. Environ. Chem. 7 (1984) 97.
[12] S. Ahmed, J. Photochem. Photobiol. A:Chem. 154 (2003) 229.
[13] K. Vinodgopal, U. Stafford, K.A. Gray, P.V. Kamat, J. Phys. Chem. 98 (1994) 6797.
[14] M.G. Kang, H.-E. Han, K.-J. Kim, J. Photochem. Photobiol. A: Chem. 125 (1999) 119.
[15] T. Hisanaga, K. Harada, K. Tanaka, J. Photochem. Photobiol. A: Chem. 54 (1990) 113.
[16] A. Mylonas, E. Papaconstantinou, J. Photochem. Photobiol. A: Chem. 94 (1996) 77.
[17] R.W. Matthews, Water Res. 5 (1986) 569.
[18] N. Peill, M.R. Hoffmann, Environ. Sci. Technol. 32 (1998) 398.
[19] N. Peill, M.R. Hoffmann, Environ. Sci. Technol. 30 (1996) 2806.
[20] S. Horikoshi, H. Hidaka, N. Serpone, Environ. Sci. Technol. 36 (2002) 1357.
[21] S. Horikoshi, A. Saitou, H. Hidaka, N. Serpone, Environ. Sci. Technol. 37 (2003) 5813.
[22] S. Horikoshi, H. Hidaka, N. Serpone, J. Photochem. Photobiol. A: Chem. 159 (2003) 289.
[23] S. Horikoshi, A. Tokunaga, H. Hidaka, N. Serpone, J. Photochem. Photobiol. A: Chem. 162 (2004) 33.
[24] S. Horikoshi, N. Serpone, H. Hidaka, Environ. Sci. Technol. 36 (2002) 5229.
[25] S. Horikoshi, H. Hidaka, N. Serpone, J. Photochem. Photobiol. A: Chem. 153 (2002) 185.
[26] S. Horikoshi, H. Hidaka, N. Serpone, J. Photochem. Photobiol. A: Chem. 161 (2004) 221.
[27] A. Loupy (Ed.), Microwaves in Organic Synthesis, Wiley-VCH Verlag, Weinheim, Germany, 2002.
[28] H.M. Kingston, S.J. Haswell (Eds.), Microwave-Enhanced Chemistry, American Chemical Society, Washington, DC, 1997.
[29] Y. Wada, H. Yin, T. Kitamura, S. Yanagida, Chem. Lett. 23 (2000) 632.
[30] R.A. Abramovitch, H. Bangzhou, M. Davis, L. Peters, Chemosphere 37 (1998) 1427.
[31] R.A. Abramovitch, H. Bangzhou, D.A. Abramovitch, S. Jiangao, Chemosphere 10 (1999) 2227.
[32] M.T. Radoiu, I. Calinescu, D.I. Martin, R. Calinescu, Res. Chem. Intermed. 29 (2003) 71.
[33] S. Horikoshi, F. Hojo, H. Hidaka, N. Serpone, Environ. Sci. Technol. 38 (2004) 2198.
[34] S. Horikoshi, H. Hidaka, N. Serpone, Chem. Phys. Lett. 376 (2003) 475.
[35] B. Kreutler, A.J. Bard, J. Am. Chem. Soc. 100 (1978) 4317.
[36] K. Harada, K. Tanaka, T. Hisanaga, S. Murata, Mizu Shori Gijutsu 26 (1985) 917.
[37] Technical Guidance for Microwave Continuous Vulcanization, Micro Denshi Co. Ltd., Saitama, Japan, 1985.
[38] (a) We should note that degradation is not faster simply because the compound that has the greater dielectric loss coefficient absorbs more microwave radiation, thus greater heat is developed. In a recent examination of various model compounds whose dielectric loss coefficients are known, we observed no trend between the dielectric loss coefficient and the dynamics of degradation in naked TiO_2 dispersions;
(b) S. Horikoshi, unpublished results.
[39] Y. Nosaka, Proceedings of the NIMS-2 International Conference, Shonan Village Center, Japan, February 1–3, 2004.
[40] (a) Y. Nosaka, S. Komori, K. Yawata, T. Hirakawa, A.Y. Nosaka, Phys. Chem. Chem. Phys. 5 (2003) 4731;
(b) T. Hirakawa, Y. Nosaka, Langmuir 18 (2002) 3247;
(c) T. Hirakawa, Y. Nakaoka, J. Nichmo, Y. Nosaka, J. Phys. Chem. B 103 (1999) 4399.
[41] P.F. Schwarz, N.J. Turro, S.H. Bossmann, A.M. Braun, A.M.A. Abdel Wahab, H. Durr, J. Phys. Chem. B 101 (1997) 7127.
[42] H. Noda, K. Oikawa, H. Kamada, Bull. Chem. Soc. Jpn. 65 (1992) 2505.
[43] M. Hajeck, Microwave catalysis in organic synthesis, in: A. Loupy (Ed.), Microwaves in Organic Synthesis, Wiley-VCH Verlag, Weinheim, Germany, 2002, pp. 345–378 (Chapter 10).
[44] R.N. Gedye, The question of nonthermal effects in the rate enhancement of organic reactions by microwaves, in: D. Clark, E. Sutton, D.A. Lewis (Eds.), Microwave: Theory and Application in Materials Processing IV, The American Ceramic Society, Ohio, 1997, pp. 165–171.
[45] R. Laurent, A. Laporterie, J. Dubac, J. Berlan, S. Lefevre, M. Audhuy, J. Org. Chem. 57 (1992) 7099.
[46] Y.Z. Steewinkel, H.L. Castricum, J. Beckers, E. Eiser, A. Bliek, J. Catal. 221 (2004) 523.
[47] D. Stuerga, P. Gaillard, Tetrahedron 52 (1996) 5505.
[48] Y.-C. Tsai, B.A. Coles, R.G. Compton, F. Marken, J. Am. Chem. Soc. 124 (2002) 9784.